International Journal of the Physical Sciences Vol. 7(1), pp. 31 - 36, 2 January, 2012
Available online at http://www.academicjournals.org/IJPS
DOI: 10.5897/IJPS11.1138
ISSN 1992-1950 ©2012 Academic Journals

Full Length Research Paper

Harmonic suppression of microstrip ring resonator using double spurlines

Niwat Angkawisittpan

Department of Electrical Engineering, Faculty of Engineering, Mahasarakham University, Mahasarakham, Thailand.
E-mail: niwat.a@msu.ac.th. Tel: +66 83 965 0011. Fax: +66 43 754 316.

Accepted 12 December, 2011

This paper presents a new design of microstrip ring resonator with harmonic suppression using double spurlines. Double spurlines are introduced for harmonic suppression in the proposed ring resonator with the purpose of circuit size miniaturization. The spurline structures force the proposed resonator to resonate only at the fundamental mode. It is shown that the harmonics can be suppressed by introducing double spurlines into the microstrip section without increasing the circuit size. The proposed resonator is designed with Finite-difference time-domain method (FDTD) and is implemented with microstrip technology. From the simulated and measured results, the proposed resonator operated in transmission mode resonates only at 2.35 GHz. Moreover, the transmission of harmonic region is reduced by 40 dB. It is appropriate to employ the proposed resonator in microwave circuit systems that require the compact size of the circuit.

Key words: Finite-difference time-domain, microstrip ring resonator, double spurlines, harmonic suppression.

INTRODUCTION

With rapid improvement and development in communication technology, there has been a great deal of demand for microwave devices for various communication applications. In the research community, microwave filters of various responses are used, for example, lowpass, highpass, bandpass and bandstop filters. In addition, microstrip ring resonator based on metamaterial structure is an alternative for microwave filters (Sharma et al., 2011). Among all the aforementioned filters, passband filters are the most widely employed. In the past, various techniques of the bandpass filter design have been proposed (Hong and Lancaster, 1995, 2001). It is not difficult to obtain desired performance of passband filters. In contrast, it is more challenging to achieve harmonic suppression. Electromagnetic interference (EMI), which is caused by harmonic radiation, is an important problem in microwave systems (Radisic et al., 1998). Many researchers focus on harmonic suppression for microwave devices because harmonic components can degrade the performance of the radio frequency (RF) front-end modules (Kim et al., 2006). To overcome the harmonic problems, various methods have been studied and published (Sung et al., 2003; Horii and Tsutsumi 1999; Sung and Kim 2005; Kwon et al., 2003; Hsiao et al., 2001). Defected ground structure (DGS) (Kazerooni and Cheldavi, 2009; Sung et al., 2003; Wang and Guan, 2011; Xiao and Zhu, 2012) and photonic band gap (PBG) (Horii and Tsutsumi, 1999; Sung et al., 2005) are the most popular solutions. In Hsiao et al. (2001), the open-circuited stub is used to suppress the harmonic components. However, the problems of DGS and PBG for harmonic suppression are that, they allow a significant backside radiation, which is harmful to the radiation characteristics of the RF front-end module such as micro-strip patch antennas. Moreover, these techniques require the fabrication of additional structures at the ground plane of the modules and increase the design complexity. Therefore, it increases the fabrication cost.

Recent developments in communication systems often require the devices with compact size, low cost, and effectiveness. Research trends in communication systems tend to invent the low cost, compact and simple fabrication of microwave devices for the modern communication devices. Therefore, compact and effective microwave devices will be very important in the future. Microstrip ring resonator is an example of microwave devices. The microstrip ring resonator is a kind of bandpass filters which can be applied in microwave filters and oscillators. It has been widely used in satellite

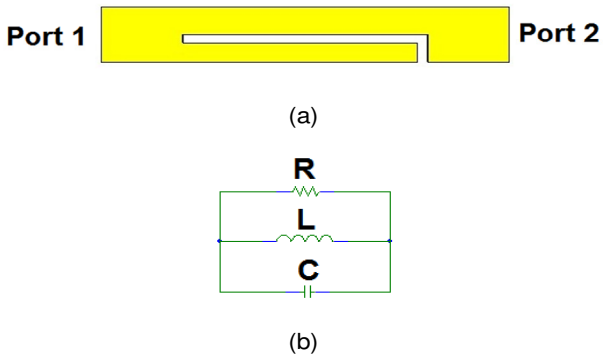

Figure 1. (a), Layout of the conventional spurline filter; (b), the equivalent circuit of the spurline filter.

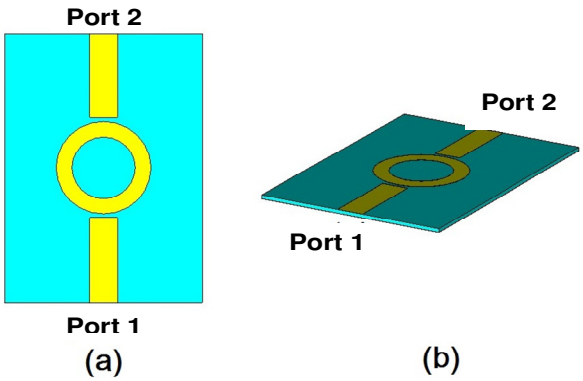

Figure 2. (a) Layout of the conventional ring resonator; (b) the isotropic view of the conventional ring resonator.

broadcast reception systems, military facilities, base stations, wireless mobile communications, telecommunications and many other areas (Vitas et al., 2010). However, EMI is still a problem in microstrip ring resonator caused by harmonic radiation.

Among the filter designs, spurline is a simple filter structure and is the smallest structure compared to other filter structures (Bates, 1977). Spurline is a simple defected structure with an L-shaped slot etched in the microstrip feed line. It can provide excellent bandstop characteristics with its compact size. Its topology and equivalent circuit are presented in Figure 1 (Liu et al., 2007).

In this paper, a promising and simple harmonic suppression with compact structure size for the microwave ring resonator is proposed. With the use of double spurlines of proper length at a suitable position on the microstrip feed line, it is clearly found that the harmonic suppression of the ring resonator can be effectively achieved. Details of the proposed design are described, and the experimental results are presented and discussed.

METHODOLOGY

This section is divided into four parts. The first explains the electromagnetic simulation technique for Maxwell's equations in order to model the proposed resonator. The second describes the design of a conventional ring resonator. The third shows the effects of the double spurlines compared to the single spurline. And the last part illustrates the proposed resonator design.

Numerical method of analysis

In the numerical analysis of the microstrip ring resonator, the Finite-difference time-domain method (FDTD) is used to simulate our design. FDTD is a simple electromagnetic simulation tool used to analyze the resonators from Maxwell's equations. The detailed theory on FDTD method is available in Taflove and Hagness (2000). A brief outline will be presented here. The first step in modeling a resonator with FDTD is to grid up the ring resonator with the number of unit cells. Then the absorbing boundary conditions are applied to cover the simulation domain. The perfectly matched layers (PML) are used as the absorbing boundary conditions in our case (Berenger, 1994). A number of parameters must be considered in order for the model to work successfully. The grid size must be small enough so that the fields are sampled sufficiently to ensure accuracy. Once the grid size is chosen, the time step is determined such that numerical instabilities are avoided according to the current stability condition.

In the simulation, the transmitted electric fields are sampled for the same polarization as the incident fields. The sampled fields in the time domain are then used to determine the transmission coefficients (S_{21}) with Fourier transformation as shown in Equation 1.

$$S_{21} = \frac{FT(E_t)}{FT(E_i)} \quad (1)$$

where FT, the Fourier transformation; E_i, incident electric fields in time domain; E_t, transmitted electric fields in time domain.

The transmission coefficient is a parameter that explains the quality of the proposed resonator. Therefore, it is very important to extract this parameter from the simulation.

Microwave ring resonators

A microwave ring resonator is a simple and narrow bandpass filter that provides the bandpass region. The simplest model of a ring resonator was first introduced by Troughton (1969). The resonant frequencies for different modes can be calculated in Equation 2.

$$f_0 = \frac{nc}{2\pi R\sqrt{\varepsilon_{eff}}} \quad (2)$$

where c is 3×10^8 m/s; n, 1, 2, 3,...; R, radius of the ring; ε_{eff}, effective permittivity of the substrate.

To illustrate the FDTD simulation, the conventional ring resonator is simulated. The configuration of the conventional ring resonator is shown in Figure 2. The ring area and feed lines are simply simulated with perfect electric conductor (PEC). The AD260A substrate is simulated with the relative permittivity $\varepsilon_r = 2.6$ and loss tangent $\tan\delta = 0.0017$. The ground plane is at the bottom layer. The length of feed line at each port is 23 mm. The width of the feed lines is 2.8 mm, which is matched to the circuit (Hong and Lancaster 2001). The average radius of the ring is 14 mm. The width of the ring is 2.8 mm. The gaps between the ring and feed lines are

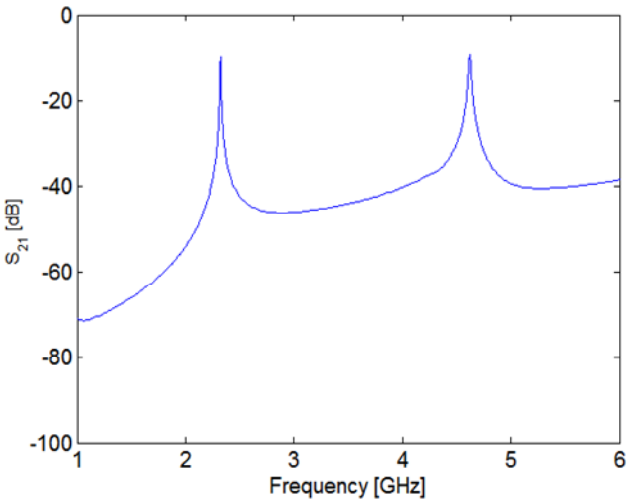

Figure 3. The simulated transmission (S_{21}) for a conventional ring resonator.

0.5 mm. Also the substrate thickness is 1 mm.

From the simulated results, Figure 3 shows the simulated transmission (S_{21}) of the conventional ring resonator. It shows that the fundamental frequency is at 2.32 GHz and the second harmonic frequency is at 4.62 GHz. The fundamental frequency obtained from the simulated result is found in good agreement with the calculation in Equation 2.

Single spurline and double spurlines

The spurline structure is a simple structure for a bandstop filter. It was introduced by Bates (1977). The desired rejected wavelength can be calculated in Equation 3.

$$\frac{\lambda_g}{4} = L \qquad (3)$$

where L, the length of the spurline; λ_g, the desired rejected wavelength in the substrate.

For a convenient way to work in the frequency domain, Equation 3 is modified here as follows:

$$f_{stop} = \frac{c}{4L\sqrt{\varepsilon_{eff}}} \qquad (4)$$

where L, the length of the spurline; ε_{eff}, effective permittivity of the substrate; c, 3×0^8 m/s; f_{stop}, the desired rejected frequency. To improve the bandstop region for the proposed resonator by spurline structure, the effects of double spurlines on transmission coefficients (S_{21}) are studied to compare with that of single spurline. The rejected frequency of a single spurline is based on the inductance value (L) and capacitance value (C) which are in parallel. Their product is LC which is inversely proportional to the rejected frequency. When two single spurlines are parallel as the double spurlines, the inductance value becomes 0.5 L and the capacitance value becomes 2 C. Consequently, their product is still LC. This confirms that the rejected frequency by double spurline structure is equal to the rejected frequency by single spurline.

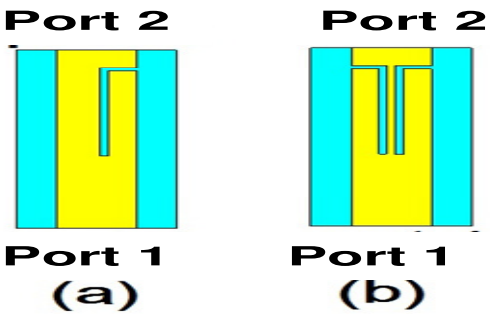

Figure 4. Configurations of spurline filters. (a) Single spurline; (b) double spurlines.

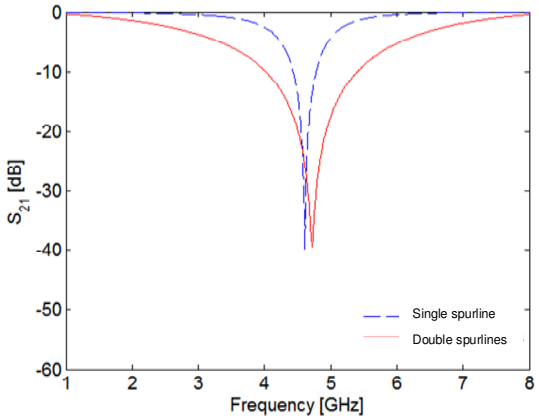

Figure 5. Comparison of simulated transmission (S_{21}) of single spurline and double spurline.

Figure 4 illustrates the double spurlines and single spurline.

To study the effects of double spurlines on transmission coefficients (S_{21}), the double spurlines are simulated using the FDTD method. In Figure 4, the microstrip feed lines are simply simulated with PEC. For both types of spurlines, the AD260A substrate is simulated with the substrate permittivity ε_r = 2.6 and loss tangent tan δ = 0.0017. The ground plane is at the bottom layer. The length of microstrip line is 23 mm. The width of the feed lines is 2.8 mm. The length of the spurlines is 11 mm. The width of the spurline microstrip is 0.6 mm. Also, the substrate thickness is 1 mm. The simulated transmissions of double spurlines and single spurline are shown in Figure 5. The simulated results show that the rejected frequencies for both double spurlines and single spurline are about 4.65 GHz. The rejected frequency obtained from simulated result is found in good agreement with the calculation in Equation 4. Also, the stopband bandwidth at -3 dB level of the double spurlines increases to about four times wider than the stopband bandwidth of the single spurline.

From the simulated results in Figure 5, the stopband bandwidth of double spurlines is very wide compared to that of single spurline. Therefore, it is very appropriate for harmonic suppression in the resonator with compact size using double spurlines.

The proposed ring resonator with harmonic suppression

We have studied the conventional ring resonator and double

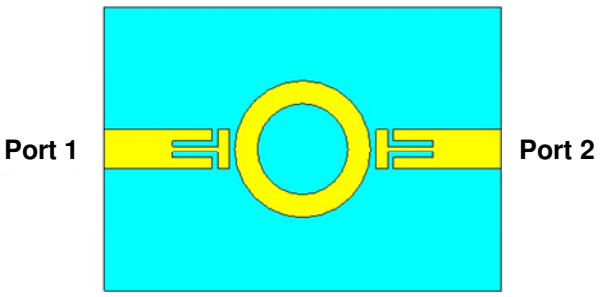

Figure 6. The sketch of the proposed ring resonator.

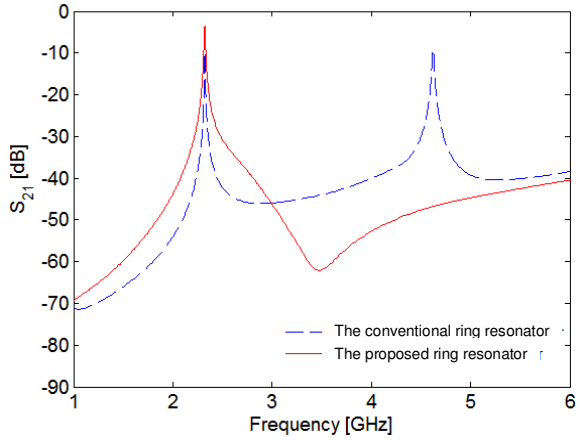

Figure 7. Comparison of simulated transmission (S_{21}) for the conventional and proposed resonators.

spurlines' effects on transmission coefficients as previously described.

Here, the proposed resonator is designed with the combination of conventional ring resonator and double spurlines. In the design, the effects of double spurlines are applied to the ring resonator for harmonic suppression. This feature makes the proposed ring resonator compact and more suitable for microwave devices compared to other techniques. Figure 6 shows the sketch of the proposed resonator prototype. The ring area and feed lines are simulated with PEC. The ground plane is at the bottom layer. The AD260A substrate is simulated with the substrate permittivity ε_r = 2.6 and loss tangent tan δ = 0.0017. The length of feed line at each port is 23 mm. The width of the feed lines is 2.8 mm. The average radius of the ring is 14 mm. The width of the ring is 2.8 mm. The gaps between the ring and feed line are 0.5 mm. The substrate thickness is 1 mm. The length of the spurlines is 11 mm. The width of the spurline microstrip is 0.6 mm. All dimensions of the prototype are used for the FDTD simulations.

Figure 7 illustrates the simulated transmission results of the conventional ring resonator and the proposed ring resonator. It can be apparently found that the harmonics can be reduced by 40 dB with the proposed ring resonator. Also, the transmission coefficients at the fundamental frequency region are improved.

The width and the length of feed lines are varied for parametric study. The width of the feed lines varied from 2.8 to 4.8 mm. From the simulated results, Figure 8 shows that the 2.8 mm width can provide the maximum transmission compared to others. This is

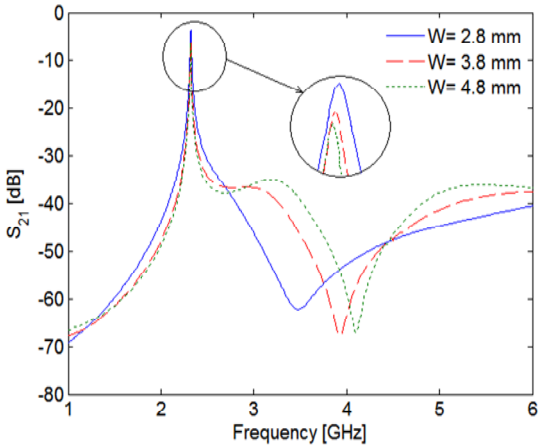

Figure 8. Comparison of simulated transmission (S_{21} from the variation of the width of the microstrip feed line.

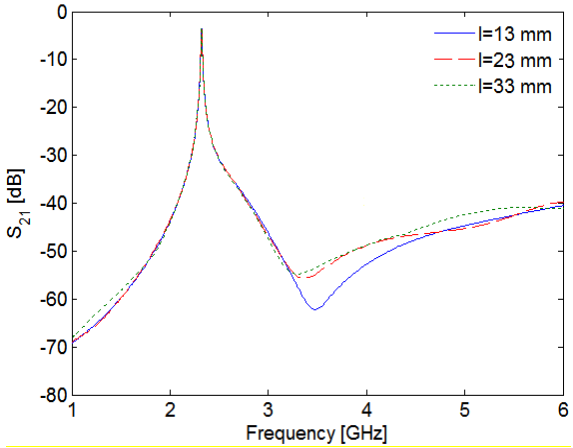

Figure 9. Comparison of simulated transmission (S_{21}) from the length variations of the feed lines with the 2.8 mm width.

because the 2.8 mm width offers characteristic impedance which match the circuit (Hong and Lancaster 2001). Therefore, the 2.8 mm width is used to determine the effects of the feed line length variations. The length of the feed lines varied from 13 to 33 mm while the width of the feed lines is fixed at 2.8 mm. Figure 9 shows that the transmission coefficients from the simulated results are rarely changed when the length of the feed lines is varied. For the purpose of compact size design, the 2.8 mm width and the 23 mm length of the feed lines are chosen to fabricate the prototype resonator.

RESULTS AND DISCUSSION

Experimental results

To validate the simulated results, the proposed resonator prototype is implemented for transmission coefficient

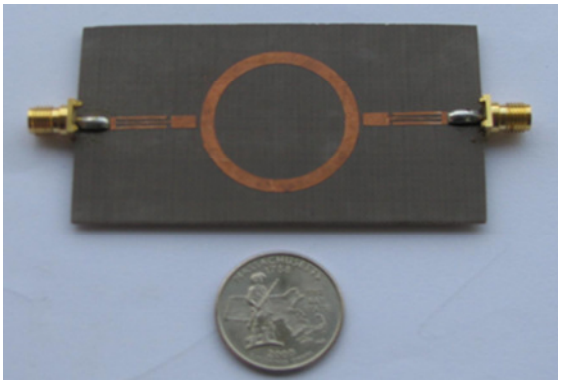

Figure 10. A photograph of the resonator prototype.

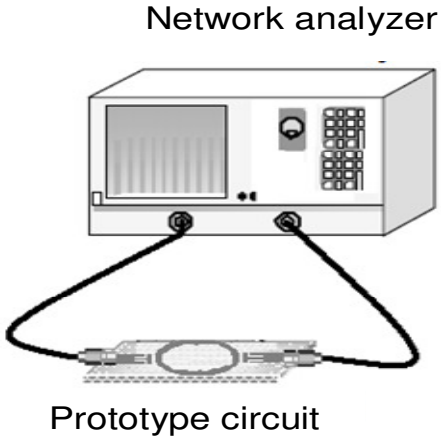

Figure 11. The sketch of the experimental setup for transmission coefficient measurement.

measurements. The proposed resonator is fabricated with the optimized dimensions previously described. Figure 10 shows a photograph of the proposed resonator prototype. The total dimensions of the prototype are 40 mm × 78 mm × 1 mm.

An Agilent HP-E5071B vector network analyzer with 50 Ω airlines is used to measure the transmission coefficients of the proposed resonator. Before the measurements of transmission coefficients are performed, the network analyzer was calibrated for the accuracy of measured results. The sketch of the measurement setup is shown in Figure 11. Ports 1 and 2 of the proposed resonator are connected to the vector network analyzer via microwave coaxial cables. Figure 12 shows the transmitted power obtained from simulations and measurements. The measured results for the proposed resonator are in good agreement with the simulated results.

It can be clearly found that the proposed resonator exhibits the fundamental frequency at 2.35 GHz and the

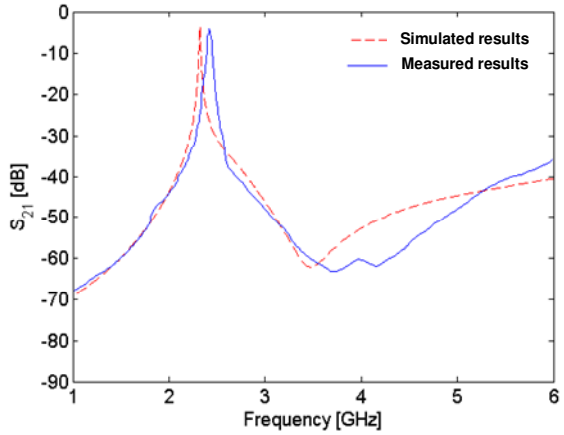

Figure 12. Simulated and measured results of the proposed ring resonator.

harmonic suppression can be achieved approximately 40 dB reduction in both simulations and measurements. Consequently, the goal of harmonic suppression in the ring resonator has been successful with the use of compact double spurlines.

Conclusion

The proposed ring resonator has been presented for harmonic suppression in the conventional ring resonator. It has been shown that the double spurlines provide the wider stopband compared to the single spurline's. Therefore, the double spurlines have been applied to the conventional ring resonator for harmonic suppression. In order to demonstrate their potential, a resonator prototype has been simulated, implemented and measured for comparison. The transmission coefficients are measured using Agilent HP-E5071B vector network analyzer. The measured results are in good agreement with the simulated results. It has been evidently shown that the proposed ring resonator provides the resonant frequency at 2.35 GHz and the double spurlines with the proper length can effectively suppress the harmonics in the ring resonator by 40 dB.

ACKNOWLEDGEMENTS

This work was granted by the Faculty of Engineering, Mahasarakham University, Mahasarakham, Thailand under the new researcher development grant.

REFERENCES

Bates RN (1977). Design of Microstrip Spur-line Band-stop Filters, IEE J. Microw. Optic. Acoust., 1(6): 209-214.
Berenger J (1994). A Perfectly Matched Layer for the Absorption of

Electromagnetic Waves. J. Comput. Phys., 114: 185-200.
Hong JS, Lancaster MJ (1995). Microstrip Bandpass Filter Using Degenerate Modes of a Novel Meander Loop Resonator. IEEE Microw. Guid. Wave Lett., 5(11): 371-372.
Hong JS, Lancaster MJ (2001). Microstrip Filters for RF/Microwave Applications. John Wiley & Sons, Inc., New York, ISBN 0-471-38877-7 2.
Horii Y, Tsutsumi M (1999). Harmonic Control by Photonic Bandgap on Microstrip Patch Antenna. IEEE Microw. Guid. Wave Lett., 9(1): 13-15.
Hsiao F, Chiou T, Wong K (2001). Harmonic Control of a Square Microstrip Antenna Operated at the 1.8 GHz Band. Proc. 2001 Asia-Pacific Microwave Conference, pp. 1052-1055.
Kazerooni M, Cheldavi A (2009). Unit Length Parameters, Transition Sharpness and Level of Radiation in Defected Microstrip Structure (DMS) and Defected Ground Structure (DGS) Interconnections. Prog. Electromagn. Res., 10: 93-102.
Kim I, Kim J, Pinel S, Laskar J, Tentzeris M, Yook J (2006). Novel Feeding Topologies for 2nd Harmonic Suppression in Broadband Microstrip Patch Antennas. Proc. 2006 IEEE Antennas Propagation Society Int. Symposium, pp. 1483-1486.
Kwon S, Lee BM, Yoon YJ, Song WS, Yook J (2003). A Harmonic Suppression Antenna for an Active Integrated Antenna. IEEE Microw. Wirel. Compon. Lett., 13(2): 54-56.
Liu H, Sun L, Shi Z (2007). Dual-bandgap Characteristics of Spurline Filters and Its Circuit Modeling. Microw. Opt. Technol. Lett., 49(11): 2805-2807.
Radisic V, Qian Y, Itoh T (1998). Novel Architectures for High-efficiency Amplifiers for Wireless Applications. IEEE Trans. Microw. Theory Technol., 46(11): 1901-1909.
Sharma V, Pattnaik SS, Garg T, Devi S (2011). A Microstrip Metamaterial Ring Resonator. Int. J. Phys. Sci., 6(4): 660-663.
Sung YJ, Kim M, Kim Y (2003). Harmonics Reduction with Defected Ground Structure for a Microstrip Patch Antenna. IEEE Antennas Wirel. Propag. Lett., 2(1): 111-113.
Sung YJ, Kim YS (2005). An Improved Design of Microstrip Patch Antennas Using Photonic Bandgap Structure. IEEE Trans. Antennas Propag., 53(5): 1799-1804.
Taflove A, Hagness S (2000). Computational Electrodynamics : The Finite-Difference Time-Domain Method (Artech House, Inc., Norwood), 2nd Edition.10: 217-219.
Troughton P (1969). Measurement Techniques in Microstrip. Electron. Lett., 5(2): 25-26.
Vitas A, Vita V, Chatzarakis GE, Ekonomou L (2010). Review of Different Ring Resonator Coupling Methods. TELE-INFO'10 Proc. The 9th WSEAS Int. Conf. Telecommunications Inform., pp. 227-231.
Wang L, Guan BR (2011). Compact Dual-Mode DGS Resonators and Filters. Prog. Electromagn. Res. Lett., 25: 47-55.
Xiao JK, Zhu YF (2012). New U-Shaped DGS Bandstop Filters. Prog. Electromagn. Res., 25: 179-191.